

# Detection of Synthetic Face Images: Accuracy, Robustness, Generalization

Nela Petrželková, Jan Čech

Faculty of Electrical Engineering, Czech Technical University in Prague

**Abstract.** An experimental study on detecting synthetic face images is presented. We collected a dataset, called FF5, of five fake face image generators, including recent diffusion models. We find that a simple model trained on a specific image generator can achieve near-perfect accuracy in separating synthetic and real images. The model handles common image distortions (reduced resolution, compression) by using data augmentation. Moreover, partial manipulations, where synthetic images are blended into real ones by inpainting, are identified and the area of the manipulation is localized by a simple model of YOLO architecture. However, the model turned out to be vulnerable to adversarial attacks and does not generalize to unseen generators. Failure to generalize to detect images produced by a newer generator also occurs for recent state-of-the-art methods, which we tested on Realistic Vision, a fine-tuned version of StabilityAI’s Stable Diffusion image generator.

## 1 Introduction

Image synthesis has made remarkable progress in recent years, thanks to the advances of generative models such as Generative Adversarial Networks (GANs) [22] and Diffusion Models [34]. Synthesized images are becoming increasingly realistic and hardly distinguishable from real ones to the naked eye of an average human and even of an expert, see Fig. 1. However, this progress also poses serious threats to individuals and society, as synthesized images, a.k.a. ‘deep fakes’ [29], can be used and have already been used for malicious purposes, such as fake porn [26], fake video calls [3,39], fake news [42], or fake videos in election campaigns [32,28]. Therefore, it is important to develop effective and robust methods to detect and expose fake images, especially in the domain of faces, which are often the target of the attacks.

In this paper, we present an experimental study in which we show some key properties of neural fake-face detectors. We use a standard classifier, and we do not primarily aim to push accuracy on standard datasets, but rather focus on other aspects of the problem. In particular, we investigate the generalization ability of the detector to unseen generators, the robustness to various image degradations and input sizes, the vulnerability to adversarial attacks, and the localization of artifacts in the case of partial manipulation of real images.

In addition to detectors which are accurate in spotting recent generator images (namely, the Stable diffusion [34] — Realistic Vision [7]), our main contribution is a thorough analysis of forgery detectors that revealed many intriguing properties. Our contributions are summarized below.

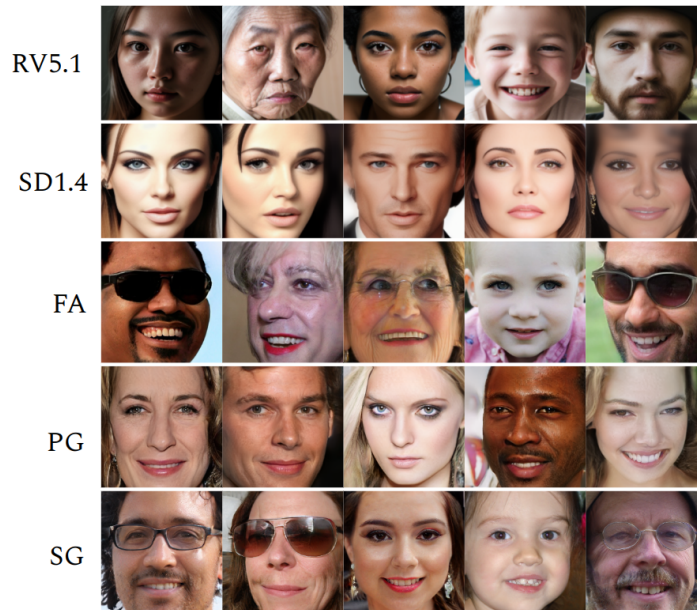


**Fig. 1.** Samples of our FF5 dataset produced by five generators: two diffusion models – Realistic Vision 5.1 [7] (RV5.1) and Stable Diffusion 1.4 [34] (SD1.4), one commercial app – FaceApp [14] (FA), two GANs – Progressive GAN [20] (PG) and StyleGAN [21] (SG).

1. **Novel FF5 dataset.** We collected a dataset of five fake face image generators. We extended DFFD corpus [10] by images produced by two recent diffusion model generators.
2. **Cross-generator-detector testing.** We show that while it is surprisingly easy to train a detector for a specific synthetic image generator, its accuracy drops dramatically when tested on images produced by a different generator, which was not trained for. This effect is partially reduced by training the detector on images generated by multiple different generators. Then, the detector generalizes better to unseen generated images. We quantify this effect and show learning curves that demonstrate the accuracy as a function of a number of training images.
3. **Robustness to input size and degradations (blur, compression) analysis.** We tested the detector against blur (reflecting input resolution), JPEG compression, and by masking the input image. The detector is surprisingly robust to the degradations and is even more robust when the degradations are added to the training set as data augmentation. For instance, our detector is able to spot synthetic images from a patch as small as  $25 \times 25$  px with accuracy about 70%.
4. **Adversarial attacks vulnerability investigation.** We demonstrate that adversarial images can be easily found and fool the detector to classify the synthetic image as real. Moreover, we show that residuals found for a particular fake image have the adversarial effect on other images and can also fool a different model of a very different architecture. We tested convolutional networks and a vision transformer.

5. **Localizing partial manipulations.** A likely scenario of a fraudulent act is to blend synthetic images into real photos. Therefore, we prepared a set of partially manipulated images using state-of-the-art inpainting models replacing key regions of the face (eyes, nose, mouth, etc.). We show that such images are easily spotted despite the manipulated area being small. Moreover, the manipulated area is localized within the image with high accuracy.

The rest of the paper is organized as follows. The related work is summarized in Sec. 2, the experimental analysis is presented in Sec. 3, and finally, Sec. 4 gives conclusions.

## 2 Related Work

In conjunction with the rapid development of high-quality synthetic image generators, research on the detection of fake images has become very active. For a comprehensive review, we refer to recent surveys [45,1,27] or a handbook [30]. In this section, we review some of the existing methods and challenges for this problem.

Historically, before the boom of deep learning, fake image detection focused on detecting “doctored images” that were manually edited or manipulated from images captured by cameras. These methods relied on various clues, such as steganographic features, compression artifacts, or inconsistencies in lighting or shadows [15,33]. However, these methods are not effective against synthetic images that are generated from scratch or with minimal human intervention.

Forensic low-level signal detectors are another class of methods. They exploit the spectral signatures of synthetic images. Inspiration probably came from the forensic recognition of a camera device [5]. More recently, researchers discovered that the residual spectra of synthetic images contain typical anomalies, which creates a spectral fingerprint of a synthetic generator [43,8,9]. A simple method based on the spectral fingerprint [12] reports a high detection accuracy. However, these methods may not be robust to image transformations, such as resizing or compression, that can alter the signal characteristics.

In a similar spirit, other more recent methods suggested that the information for fake image detection is deeply embedded in the image signals and can be detected independently of the image content. Work [4] proposed a method that uses a convolutional neural network with a narrow receptive field to detect fake images from signal patches, and showed that some regions, such as hair, are more discriminative than others.

Another paper [43] has shown that the detection of synthetic images generated by GANs is relatively easy, as they exhibit certain distinctive features and a standard CNN classifier can be easily trained to capture this difference. The paper even shows a good generalization ability, in case the model is tested on images produced by a generator for which it was not trained for. However, they used only GAN-based generators. In this paper we will show that the generalization of detectors to unseen generators between recent models (especially of different architectures GANs/diffusion models) is poor. We show that recent state-of-the-art synthetic image detectors fail completely when tested on images produced by novel unseen generators.

Besides detection, some recent works have also addressed the localization of fake images, which aims to segment the manipulated areas of the real images. The problem is challenging considering possibly a small area of manipulation. Some methods do not use any special architecture for localization, but rely on post-processing techniques. Recent paper [38] compares a popular Grad-CAM [35] to highlight the regions that contribute to the classification decision and the scanning technique of [4] to localize synthetic regions in partially manipulated images. Other methods use more complex architectures, such as multi-branch network [17], or dense self-attention network [18], to explicitly learn the localization maps. Paper [25] fine-tunes a large segmentation model (SAM) [24] to adapt it to the fake image domain. We show that precise localization results are achieved for relatively small regions using a simple YOLO-based architecture [31], namely YOLOv8 [41], as long as the fake images are composed of images produced by the same generator model that we trained on.

Deep neural networks are known to be vulnerable to adversarial attacks [37], which are small imperceptible perturbations of the input that cause a network to make a wrong prediction. This problem has been extensively studied in various domains, such as image classification [16], object detection [44], or face recognition [11]. In this paper, we show that this vulnerability also applies to the fake image detection domain and that a common way of generating adversarial examples can fool the detectors into classifying fake images as real.

### 3 Experimental Analysis

Our FF5 dataset consists of face images produced by five generators; see Fig. 1. We use two diffusion models: Realistic Vision V5.1 [7] (RV5.1), which is fine-tuned Stable Diffusion sharing the same architecture, and official StabilityAI’s Stable Diffusion V1.4 [34] (SD1.4). Then three synthetic sets that are part of the DFFD corpus [10]: FaceApp [14] (FA), which are images produced by a popular commercial mobile phone application with undisclosed technology, and GANs PG-GAN2 [20] (PG), and StyleGAN [21] (SG).

For the diffusion models, we used dynamic prompting [13] which enables us to automatically alter a prompt with terms from predefined options. Our base prompt was “RAW photo” and we randomly altered it with attributes influencing the gender, age, accessories, and the environment. See Sec. 3.5 for more details. That enabled us to quickly generate diverse images. With different random seeds, we generated almost 1.7k images for each diffusion model. The other generators consist of 2k images for each of FA, PG, and SG.

For the negative class of real images, we use images from the FFHQ dataset [21]. All synthetic and real images underwent the same preprocessing procedure, cropping with the same margin, aligning using facial landmarks, and resampling to  $224 \times 224$  px.

#### 3.1 Cross-generator testing

In this experiment, we trained the ResNET-50 backbone binary classifiers [19] between synthetic and real samples. This is the same architecture used by [43]. The dataset was

**Table 1.** Cross-generator testing. Each cell (*row, col*) shows test accuracy in percent of the models trained (a) on generator *row* / (b) all without generator *row*, tested on generator *col*.

		Test set				
		RV5.1	SD1.4	FA	PG	SG
Training set	RV5.1	<b>100</b>	58	49	50	50
	SD1.4	51	<b>100</b>	50	54	49
	FA	53	50	<b>80</b>	87	60
	PG	49	61	54	<b>100</b>	50
	SG	48	48	54	66	<b>94</b>

(a) Training on a single generator

		Test set				
		RV5.1	SD1.4	FA	PG	SG
Training set	-RV5.1	<b>58</b>	92	80	94	91
	-SD1.4	91	<b>84</b>	85	91	91
	-FA	95	94	<b>55</b>	94	89
	-PG	93	92	77	<b>79</b>	85
	-SG	95	95	80	94	<b>52</b>

(b) Leave one out training

always split to 80-10-10% for disjoint training-validation-test sets, respectively. The ratio between synthetic and real classes was always 50-50%. We used Adam optimizer with default settings and horizontal flipping as data augmentation. We always selected the model that achieved the best accuracy on the validation set.

We performed the following cross-generator experiment. We first trained on single-generator images and tested on all in the set, see Tab. 1a. Then, the other way around, we trained on all generators with one left out and tested again on all, see Tab. 1b.

We can see in Tab. 1a that if the detector is trained on the same model as it is tested (diagonal of the table), the accuracy is perfect for RV5.1, SD 1.4, PG, and very high for SG. The accuracy is only 80% for FA. FA, FaceApp [14], a commercial app with unknown technology behind, probably blends the real face with some manipulations, making it harder to identify. However, we can clearly see (off the diagonal) that accuracy drops close to chance when we test on images produced by models for which the detector was not trained on. Interestingly, this is not the case of FA, which achieves even higher accuracy on PG, which might indicate similar technology, but the converse is not true. The generalization does not occur for even very similar models, the diffusion models RV5.1 and SD 1.4 share the same architecture. The first is a fine-tuned version of the latter.

In Tab. 1b, when the detector is trained on multiple models, a certain level of generalization to unseen generators is achieved for some models, as seen in the diagonal now. SD1.4 seems to generalize well while it was not trained on it. However, RV5.1 is similar to SD1.4, but the generalization is not reciprocal. PG seems to generalize too, and the rest is close to chance.

We see that the detector generalization to an unseen model is a problem. Therefore, in the following experiment, we measure how many samples of the new generator are needed for fine-tuning. We always start from the model that is trained on all the generators of our set except one (i.e., the rows of Tab. 1b), so its initial accuracy is on the diagonal of Tab. 1b. Then we gradually add training samples of the new model (0, 5, 10, 50, 100, 500, 1000, 1666) samples and measure the accuracy on the test set. The results are shown as learning curves in Fig. 2. Note that the plot has a logarithmic horizontal axis.

Interestingly, for some generators, only units or small tens of training samples are needed to significantly improve detection accuracy.

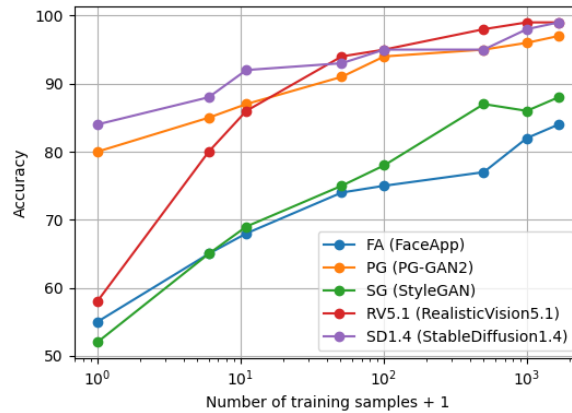


**Fig. 2.** Learning curves for training a detector to spot images produced by a new generator. Test accuracy as a function of the number of training samples. Horizontal axis is logarithmic.

**Table 2.** Comparison with the state of the art. Accuracy on test set produced by RV5.1 generator. Last two models were trained on independent split of RV5.1 dataset.

Model	Wang 2020 [43]	HiFi 2023 [17]	Durrall 2019 [12]	ResNET-50 (ours)
Accuracy	48.3	44.2	87.7	99.5

*Comparison with the state of the art.* We evaluate recent fake image detectors on our test set produced by RV5.1 generator. We tested Wang 2020 [43], HiFi 2023 [17], which both provide pre-trained models, and Durrall 2019 [12] which we trained on the independent training split of the RV5.1 dataset by using the training script provided by the authors. Our ResNET-50 was trained on the same set.

The results are shown in Tab. 2. Although Wang 2020 [43] claimed to generalize to unseen generators, it no longer holds with novel generators – the diffusion model RV5.1. The model achieved accuracy close to chance. It was trained on GAN-based generators which does not provide any generalization to the recent diffusion RV1.5 generator. Moreover, the recent HiFi 2023 [17] also failed, despite being trained on diffusion models. It achieves low accuracy 44.2% as it confused almost all RV5.1 images with real ones, while classifying some of the real images as synthetic. This generalization failure is particularly striking, as this method presented in the last CVPR conference is supposed to be the state of the art. This finding reveals the difficulty of the problem of detecting unseen generators.

Durrall 2019 [12] resulted in an inferior accuracy compared to our model. The reason is probably that it uses very simple features, magnitude spectrum radius and logistic regression.

### 3.2 Detector accuracy for input degradation

Since the image may be distorted, e.g., resized, compressed, cropped, prior to the distribution, we measured detector accuracy for the distortion. Gaussian blur simulates shrinking the resolution, and JPEG a lossy compression. The size of the input was simulated by masking the input image – a square patch of a given size at random position is kept, while all other pixels are replaced with zeros in all three RGB channels. See Fig. 4 for some examples.

We evaluated two scenarios. First, we tested the original model, which was trained on undistorted images from the RV5.1 set. Second, we re-trained the detector with the image degradation as data augmentation.

The results are shown in Fig. 3. We can see that the detector proves a good robustness to the degradations, especially for the second scenario with re-training. For instance, the detector achieves accuracy about 80% for Gaussian blur  $\sigma = 17$  px, 90% for JPEG quality 10, and 70% for a patch as small as  $25 \times 25$  px.

### 3.3 Adversarial attacks

In this section, we study the vulnerability of our detector to adversarial attacks. An adversarial attack means performing a hardly perceptible modification of an image (residue) that causes a change in classification of the detector, i.e., a synthetic image is classified as real. First, we find the adversarial residua for a given image. We use the simple fast gradient sign method (FGSM) [16]. The adversarial residuum is then an image of the same size as the input receptive field of the model that contains signs of the gradient of the output class score with respect to the input pixel intensities in each channel. This is easily calculated by backpropagation without any optimization.

We tested the attacks on three different architectures of detectors: ResNET-50 [19], Xception [6], ViT-tiny [40], which we trained on our training set RV5.1. Two of the models is of perfect 100% accuracy on the test set, ViT-tiny achieved 83%.

The resulting residua are shown in Figs. 5 and 6. The residua are scaled up multiple times in the figures, otherwise the pattern would not be visible. All these residua scaled by strength  $\epsilon$  if summed with the original images will switch the classification of the corresponding detector to “real”. Residua for different models appear different and the pattern is visibly influenced by the structure of the original image, as seen in Fig. 6.

We then tested whether the residua found for a specific image and a specific detector act adversarially on another image for the same or a different detector model. We measured the success of attacks by the confusion rate, which depicts a percentage of test cases when the model switched the classification due to the attack from “fake” to “real” over the number of “fake” decisions prior to the attack.

First, we performed the cross-sample test, where the adversarial residua are found for a given image and are tested also on different images. This was done for the three models separately. The confusion rates for increasing strength of the residua  $\epsilon$  are presented in Tab. 3. Cross-sample attacks are seen to work and are more successful with greater strength  $\epsilon$ . We show this experiment as an interesting insight, although this scenario is not so relevant practically, since an attacker would prepare an optimum residue right for his fake image.

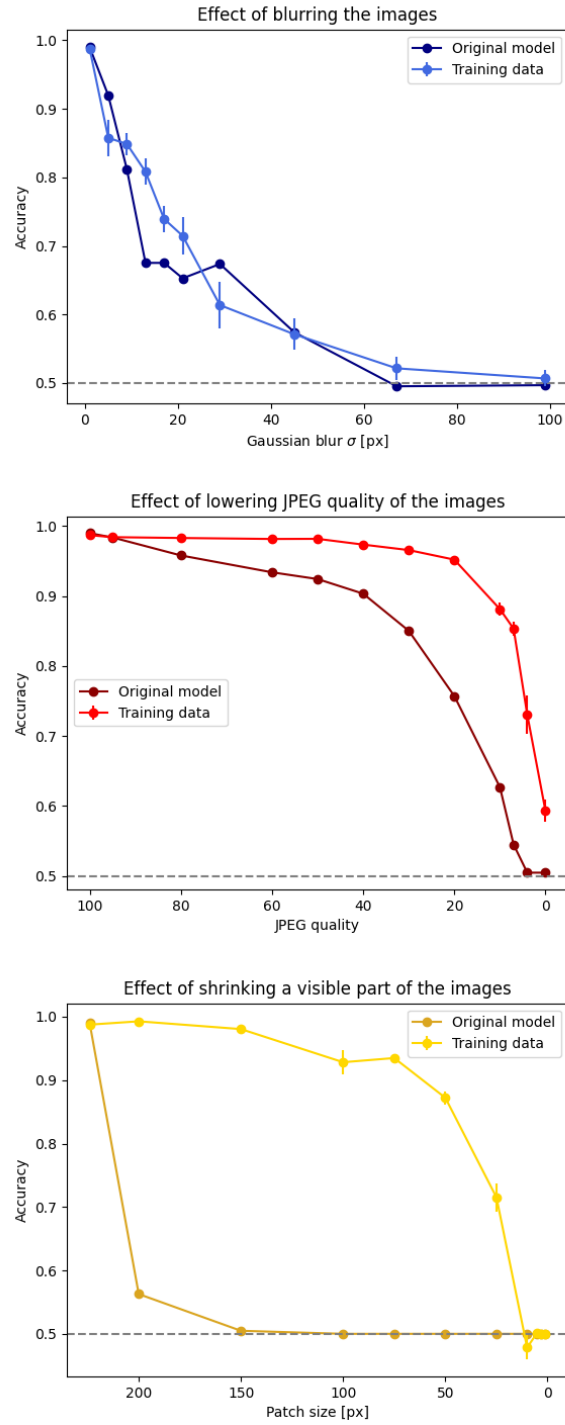


**Fig. 3.** Detector accuracy for input degradation. From top to bottom: Gaussian blur, JPEG compression, input patch size. Two scenarios are tested: (1) the detector is trained on undistorted images only, (2) the detector is trained on images including the degradations. Plots have error bars of standard deviation across 10 training trials.

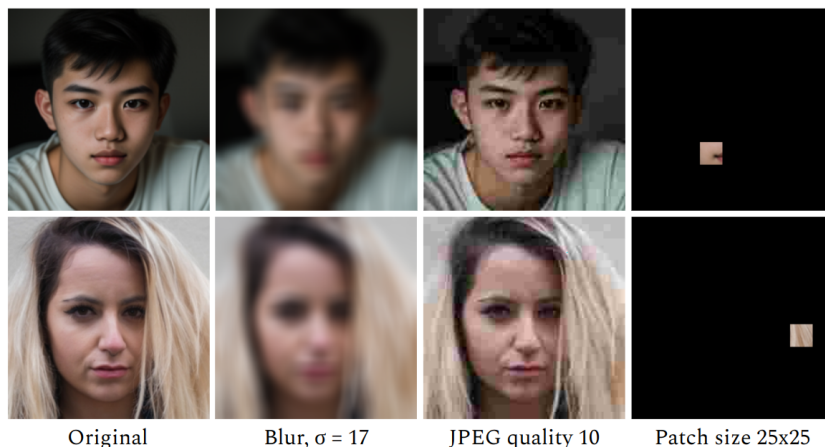


**Fig. 4.** Examples of distorted images.

Much more important is the cross-model scenario, where the adversarial residua are found for a given image and a given model, and are tested also on other models of different architectures. The results for increasing strength of the residua  $\epsilon$  are summarized in Tab. 4.

We see that for a small strength  $\epsilon = 0.01$ , in-model attacks (in the diagonal) are successful for ResNET-50 and Xception. However, for higher strength, cross-model attacks, where a model of *different architecture unknown by the attacker* works also, as seen off the diagonal. For strength  $\epsilon = 0.05$  a residue found for ViT-tiny confuses ResNET-50 and Xception too.

**Table 3.** Cross-sample adversarial attacks. Adversarial residua found for a given image were tested on different images. Table show confusion rate for increasing strength of residua  $\epsilon$ . The experiment was done separately for three model architectures.

	$\epsilon = 0.01$	$\epsilon = 0.02$	$\epsilon = 0.05$
ResNET-50	2.20	67.40	100.00
Xception	96.34	100.0	100.00
ViT-tiny	8.63	25.88	97.25

### 3.4 Localizing partial manipulations

A likely scenario for constructing a fake image is that a synthetic image is seamlessly blended into a real face image. In this experiment, we will show that these partial manipulations are easy to identify together with localizing the area of the manipulations.

We first prepared a dataset of partially manipulated face images. We randomly sampled real faces (from the FFHQ dataset) and, for each image, uniformly changed either

**Table 4.** Cross-architecture adversarial attacks for increasing strength of the residua  $\epsilon$ . Each cell ( $row, col$ ) corresponds to confusion rate in percent. The attack was targeted against model of architecture in  $row$  and tested against the model of architecture in  $col$ .

<b>FGSM</b> $\epsilon = 0.01$	ResNET-50	Xception	ViT-tiny
ResNET-50	<b>100.00</b>	67.15	7.30
Xception	2.55	<b>100.00</b>	6.93
ViT-tiny	0.39	6.64	<b>59.77</b>

<b>FGSM</b> $\epsilon = 0.02$	ResNET-50	Xception	ViT-tiny
ResNET-50	<b>100.00</b>	100.00	8.76
Xception	48.54	<b>100.00</b>	8.39
ViT-tiny	16.80	89.06	<b>92.97</b>

<b>FGSM</b> $\epsilon = 0.05$	ResNET-50	Xception	ViT-tiny
ResNET-50	<b>100.00</b>	100.0	15.69
Xception	100.00	<b>100.0</b>	10.22
ViT-tiny	100.00	100.0	<b>100.0</b>

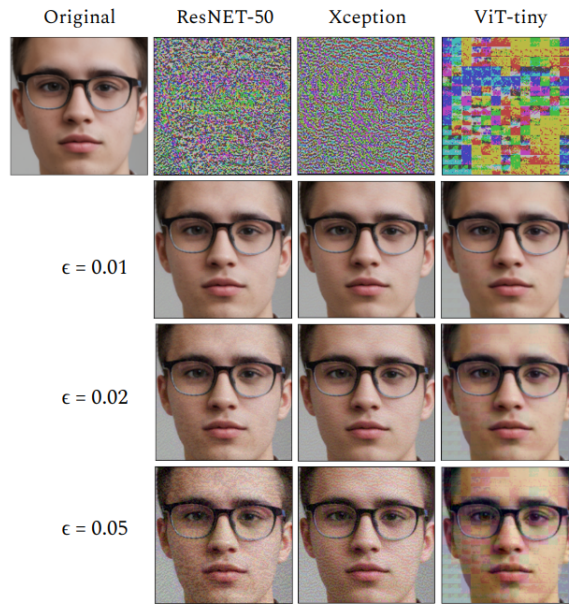


**Fig. 5.** Adversarial images crafted to confuse the classification model. They are created by summing the original (top left) image with adversarial residue (top row) scaled by  $\epsilon$ . Results shown for three models (ResNET-50, Xception, ViT-tiny) with increasing strength  $\epsilon$ .

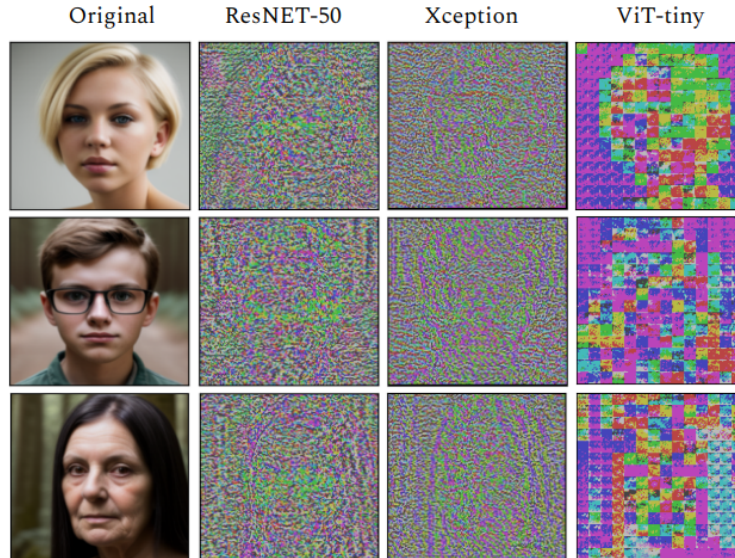


**Fig. 6.** Other examples of adversarial residua shown for input images and three fake detector models (ResNET-50, Xception, ViT-tiny).

of the eyes, eyebrows, nose, or mouth. These regions were detected using facial landmarks [23], and the change of content within the region was carried out by Stable Diffusion inpainting [34]. This way we produced a dataset of 3.2k partially manipulated images that were mixed with 540 real images.

The data set was divided into training, validation, and test subsets with proportions of 80%, 16%, and 4%, respectively. Then, we trained YOLOv8 [41], which is a YOLO-based architecture [31] with a segmentation head.

Qualitative results on the test set are shown in Fig. 7. It is seen that detected regions are found precisely, despite the fact that the manipulated (synthetic region) is sometimes fairly small with respect to the entire (real) image and no obvious artifacts are visible in the images.

Quantitatively, the detector achieved mAP50 98% (mean average precision for 50% prediction/ground-truth detection overlap by intersection over the union). Pixelwise recall and precision were 95% and 91%, respectively.

We compared the detector with HiFi [17] which is supposed to provide localization of the manipulation. However, this detector failed completely and always recognized all our partially manipulated images as real. This again confirms, similarly to our findings in Sec. 3.1, that generalization to localize partial manipulations when using unseen models is very challenging.

*Localization accuracy as a function of manipulated area size.* In this experiment, we quantify how the size of the manipulated area impacts the localization accuracy of our YOLOv8s-seg segmentation model. We created a dataset consisting of 4.5k of partially



**Fig. 7.** Localizing partial image manipulations perpetrated by inpainting of the ground-truth (GT) regions for examples of the test set. Localization predictions were found by our YOLOv8-based model.

manipulated images with various sizes of the manipulated area. In particular, we randomly sampled real (FFHQ dataset) images, then for each image, we generated the manipulated area by a randomly placed, rotated, and cropped ellipse of random size. Finally, as in the previous experiment, we used Stable Diffusion’s inpainting to modify the images in these areas. Several examples can be seen in Fig. 8a. The model was trained on 2.7k of the 4.5k images, 1.8k were used for validation and testing.

The test set was split into equally sized bins Q1–Q4 according to the size of the manipulated areas: ‘Q1’: (0, 0.08), ‘Q2’: (0.08, 0.16), ‘Q3’: (0.16, 0.25), ‘Q4’: (0.25, 0.36), where the numbers denote a ratio of the area of the generated parts with respect to the total area. The results are shown in Fig. 8b, where mAP50 is evaluated for each test set bin. We can see that it is obviously easier to localize larger areas for the model. Unlike in previous experiments, where we modified facial features (face, eyes, eyebrows, nose, mouth), here we chose the unpainted regions completely randomly. It happens that especially small regions are located in flat areas without texture. These regions do not manifest much of a usable signal for identification as do larger areas. This can be the reason why the smaller modified areas are more challenging to localize by the model.

### 3.5 Implementation details

We used AUTOMATIC1111’s Stable Diffusion Web UI [2] for our experiments. Besides graphical interface with many plugins, it provides a convenient batch processing.

To generate our dataset (RV5.1 and SD1.4), we used dynamic prompt [13]. This is the Web UI extension that implements an expressive template language for the generation of random or combinatorial prompts. In particular, we used the following prompt to get diversity in our dataset: “RAW photo, {older | younger} {man | woman | lady | girl | boy} { {smiling | staring} | with glasses | with hat | with {brown | blonde | dark} {straight | curly | short} hair }, high quality portrait taken with Nikon camera, in {na-

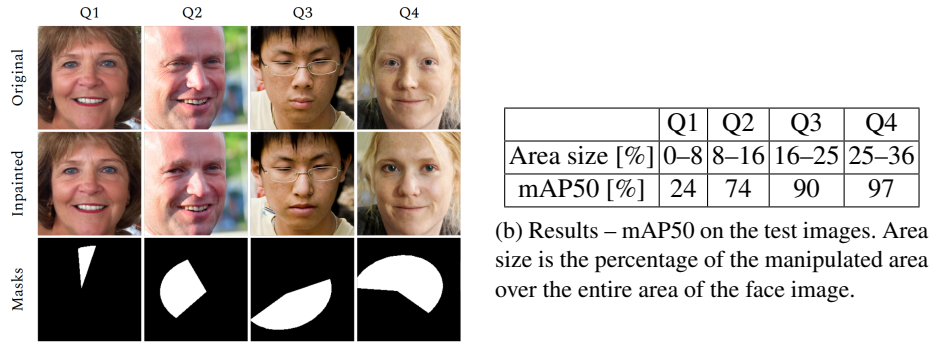


**Fig. 8.** Localization accuracy as a function of manipulated area size.

ture | a city | a room | an office | a park | a street | a forest }”. All models were trained with PyTorch framework.

## 4 Conclusion

We collected the FF5 dataset that includes images of recent diffusion generators. We conducted an extensive experimental study on the detection of synthetic face images. We will make our dataset and models publicly available. Our results allow us to draw the following conclusions.

The *good news* is that it is possible (if the generator of synthetic images is available) to train a simple model with an off-the-shelf architecture, which has almost perfect accuracy in distinguishing between synthetic and real images. The accuracy achieved far outperforms human abilities [36]. Another positive aspect is that the detector can be trained with data augmentation, to make it robust to common image distortions (reduced resolution, compression), and it can achieve good accuracy with only a small input patch from the face. Moreover, it is easy to detect the case of partial manipulations, where a collage of real and synthetic images is made. The manipulated area is automatically localized by training a standard model [41].

However, there are also *bad news*. It is simple to prepare an adversarial attack. It turns out that the residua found for a target model act adversarially, even on other models of very different architectures. We showed that adversarial images found for vision transformers often confuse convolutional networks. The worst news is that the detectors do not generalize well to generators they were not trained on. This is not just the case of our simple detector, but we showed that two tested state-of-the-art detectors failed completely and could not detect synthetic images generated by a newer generator, which they were not trained on.

These bad news demonstrate that universal detection of synthetic/fake images is a very tough problem, which is far from being solved despite active research in recent times.

## References

1. Akhtar, Z.: Deepfakes generation and detection: A short survey. *Journal of Imaging* **9**(1), 18 (2023)
2. AUTOMATIC1111: Stable Diffusion Web User Interface (2023), GitHub repository, <https://github.com/AUTOMATIC1111/stable-diffusion-webui>
3. Bloomberg news: The next wave of scams could be deepfake video calls from your boss (Aug 30, 2023), <https://www.linkedin.com/pulse/next-wave-scams-could-deepfake-video-calls-from-your-boss/>
4. Chai, L., Bau, D., Lim, S.N., Isola, P.: What makes fake images detectable? understanding properties that generalize. In: Proc. ECCV (2020)
5. Chen, M., Fridrich, J., Goljan, M., Lukás, J.: Determining image origin and integrity using sensor noise. *IEEE Transactions on information forensics and security* **3**(1), 74–90 (2008)
6. Chollet, F.: Xception: Deep learning with depthwise separable convolutions. In: Proc. CVPR (2017)
7. CivitAI: Realistic vision, v5.1 (2023), <https://civitai.com/models/4201/realistic-vision>
8. Corvi, R., Cozzolino, D., Zingarini, G., Poggi, G., Nagano, K., Verdoliva, L.: On the detection of synthetic images generated by diffusion models. In: Proc. ICASSP (2023)
9. Corvi, R., Cozzolino, D., Poggi, G., Nagano, K., Verdoliva, L.: Intriguing properties of synthetic images: from generative adversarial networks to diffusion models. In: Proc. CVPR, pp. 973–982 (2023)
10. Dang, H., Liu, F., Stehouwer, J., Liu, X., Jain, A.: On the detection of digital face manipulation. In: Proc. CVPR (2020)
11. Dong, Y., Su, H., Wu, B., Li, Z., Liu, W., Zhang, T., Zhu, J.: Efficient decision-based black-box adversarial attacks on face recognition. In: Proc. CVPR (2019)
12. Durall, R., Keuper, M., Pfrendt, F.J., Keuper, J.: Unmasking deepfakes with simple features. arXiv preprint arXiv:1911.00686 (2019)
13. Eyal, A.: Stable Diffusion Dynamic Prompts extension (2023), <https://github.com/adieyal/sd-dynamic-prompts>
14. FaceApp Technology Limited: Faceapp (2023), <https://www.faceapp.com/>
15. Farid, H.: Image forgery detection. *IEEE Signal processing magazine* **26**(2), 16–25 (2009)
16. Goodfellow, I.J., Shlens, J., Szegedy, C.: Explaining and harnessing adversarial examples. In: Proc. ICLR (2015)
17. Guo, X., Liu, X., Ren, Z., Grosz, S., Masi, I., Liu, X.: Hierarchical fine-grained image forgery detection and localization. In: Proc. CVPR (2023)
18. Hao, J., Zhang, Z., Yang, S., Xie, D., Pu, S.: Transforensics: image forgery localization with dense self-attention. In: Proc. International Conference on Computer Vision (2021)
19. He, K., Zhang, X., Ren, S., Sun, J.: Deep residual learning for image recognition. In: Proc. CVPR (2016)
20. Karras, T., Aila, T., Laine, S., Lehtinen, J.: Progressive growing of GANs for improved quality, stability, and variation. In: Proc. ICLR (2018)
21. Karras, T., Laine, S., Aila, T.: A style-based generator architecture for generative adversarial networks. In: Proc. CVPR (2019)
22. Karras, T., Laine, S., Aittala, M., Hellsten, J., Lehtinen, J., Aila, T.: Analyzing and improving the image quality of StyleGAN. In: Proc. CVPR (2020)
23. King, D.E.: Dlib-ml: A machine learning toolkit. *Journal of Machine Learning Research* **10**, 1755–1758 (2009)
24. Kirillov, A., Mintun, E., Ravi, N., Mao, H., Rolland, C., Gustafson, L., Xiao, T., Whitehead, S., Berg, A.C., Lo, W.Y., et al.: Segment anything. arXiv preprint arXiv:2304.02643 (2023)

25. Lai, Y., Luo, Z., Yu, Z.: Detect any deepfakes: Segment anything meets face forgery detection and localization. In: Proc. CCBR (2023)
26. Lee, D.: Deepfakes porn has serious consequences. BBC News (Feb 3, 2018), <https://www.bbc.com/news/technology-42912529>
27. Mary, A., Edison, A.: Deep fake detection using deep learning techniques: A literature review. In: Proc. IEEE International Conference on Control, Communication and Computing (ICCC) (2023)
28. Meaker, M.: Slovakia's election deepfakes show AI is a danger to democracy. Wired (Oct 3, 2023), <https://www.wired.co.uk/article/slovakia-election-deepfakes>
29. Nguyen, T.T., Nguyen, Q.V.H., Nguyen, D.T., Nguyen, D.T., Huynh-The, T., Nahavandi, S., Nguyen, T.T., Pham, Q.V., Nguyen, C.M.: Deep learning for deepfakes creation and detection: A survey. *Computer Vision and Image Understanding* **223**, 103525 (2022)
30. Rathgeb, C., Tolosana, R., Vera-Rodriguez, R., Busch, C.: Handbook of digital face manipulation and detection: from DeepFakes to morphing attacks. Springer Nature (2022)
31. Redmon, J., Divvala, S., Girshick, R., Farhadi, A.: You only look once: Unified, real-time object detection. In: Proc. CVPR (2016)
32. Reuters: Erdogan rival accuses Russia of 'deep fake' campaign ahead of presidential vote (May 12, 2023), <https://www.reuters.com/world/middle-east/erdogan-rival-accuses-russia-deep-fake-campaign-ahead-presidential-vote-2023-05-12/>
33. Rocha, A., Scheirer, W., Boulton, T., Goldenstein, S.: Vision of the unseen: Current trends and challenges in digital image and video forensics. *ACM Computing Surveys (CSUR)* **43**(4), 1–42 (2011)
34. Rombach, R., Blattmann, A., Lorenz, D., Esser, P., Ommer, B.: High-resolution image synthesis with latent diffusion models. In: Proc. CVPR (2022)
35. Selvaraju, R.R., Cogswell, M., Das, A., Vedantam, R., Parikh, D., Batra, D.: Grad-CAM: Visual explanations from deep networks via gradient-based localization. In: Proc. ICCV (2017)
36. Somoray, K., Miller, D.J.: Providing detection strategies to improve human detection of deepfakes: An experimental study. *Computers in Human Behavior* **149**, 107917 (2023)
37. Szegedy, C., Zaremba, W., Sutskever, I., Bruna, J., Erhan, D., Goodfellow, I., Fergus, R.: Intriguing properties of neural networks (2014)
38. Tantaru, D., Oneata, E., Oneata, D.: Weakly-supervised deepfake localization in diffusion-generated images. In: Proc. WACV (2024), to Appear
39. The Guardian: European politicians duped into deepfake video calls with mayor of Kyiv (Jun 25, 2022), <https://www.theguardian.com/world/2022/jun/25/european-leaders-deepfake-video-calls-mayor-of-kyiv-vitali-klitschko>
40. Touvron, H., Cord, M., Douze, M., Massa, F., Sablayrolles, A., Jégou, H.: Training data-efficient image transformers & distillation through attention. *CoRR* **abs/2012.12877** (2020), <https://arxiv.org/abs/2012.12877>
41. Ultralytics: Yolo v8. GitHub repository (2023), <https://github.com/ultralytics/ultralytics>
42. Wakefield, J.: Deepfake presidents used in Russia-Ukraine war. BBC News (March 18, 2022), <https://www.bbc.com/news/technology-60780142>
43. Wang, S.Y., Wang, O., Zhang, R., Owens, A., Efros, A.A.: CNN-generated images are surprisingly easy to spot...for now. In: Proc. CVPR (2020)
44. Wei, X., Liang, S., Chen, N., Cao, X.: Transferable adversarial attacks for image and video object detection. In: Proc. International Joint Conference on Artificial Intelligence. AAAI Press (2019)
45. Zanardelli, M., Guerrini, F., Leonardi, R., Adami, N.: Image forgery detection: a survey of recent deep-learning approaches. *Multimedia Tools and Applications* **82**(12), 17521–17566 (2023)